The International Journal of Advanced Manufacturing Technology (2022) 120:7547–7563
https://doi.org/10.1007/s00170-022-09210-3

ORIGINAL ARTICLE

Multi-objective optimization of directed energy deposition process by using Taguchi-Grey relational analysis

Yu-Yang Chang[1] · Jun-Ru Qiu[1] · Sheng-Jye Hwang[1]

Received: 6 February 2022 / Accepted: 8 April 2022 / Published online: 29 April 2022

Abstract
In this study, a multi-objective optimization of directed energy deposition (DED) process was conducted with Taguchi-Grey relational analysis. The used part was designed as a flat rectangle which would be deposited by a single-layer and multi-track DED process. Firstly, after finishing Taguchi experiments, the effects of five control factors (laser power, overlap ratio, powder feed rate, scanning speed and laser defocus distance) on three DED product qualities (cladding efficiency, surface roughness and porosity) were, respectively, analyzed. Then, through Grey relational analysis (GRA), an optimal factor setting which can take all qualities into account was found and had better deposition results compared with previous setting. Furthermore, ANOVAs were conducted to find out significant factors of each qualities. By using the significant factors as variations, three second-order polynomial regression predictive models for qualities were created. Based on the GRA and ANOVAs results, additional one-factor-at-a-time (OFAT) experiments which used the optimal setting as the center point were performed. The qualities variation resulting from adjusting overlap ratio and laser defocus distance of optimal setting were investigated, and the results were also used as additional data to verified the accuracies of three regression models.

Keywords Directional energy deposition · Taguchi-Grey relational analysis · Cladding efficiency · Surface roughness · Porosity

1 Introduction

DED is a metal additive manufacturing technology. It uses powder feeding gas to transport metal powder to the energy center of heat source and the melted powder directly deposited on a substrate or surface of an unfinished part. By repeating the deposition layer by layer, a 3D product can be fabricated by DED.

Because of numerous advantages such as short production period, material saving, good mechanical properties of products and the ability to produce parts with complex geometry, DED frequently be used in various fields in recent years. However, DED has many control factors that can affect product qualities such as cladding efficiency, surface roughness and porosity. Above three qualities, respectively, have great influences on processing time and cost of manufacturing, products surface topography and products strength. So, to realize how factors affect qualities and to obtain better qualities which user need are the important research goals of DED flied.

Kuriya et al. [1] pointed out that high energy input can prolong the solidification time melt pool requiring, thereby reducing the voids of products. Base on Liu et al. [2] research results, surface roughness increased if laser energy density was too high or too low. However, porosity rose sharply (>5%) when laser energy density was too high. It was considered resulting from that excessive energy caused thermal residual stress and made internal fractures. Li and Ma [3] established a model to simulate the cross section shape of single-layer and multi-track DED part, and revealed

Yu-Yang Chang, Jun-Ru Qiu and Sheng-Jye Hwang contributed equally to this work.

✉ Sheng-Jye Hwang
jimppl@mail.ncku.edu.tw

Yu-Yang Chang
tonyany09@gmail.com

Jun-Ru Qiu
kevin94047@gmail.com

[1] Department of Mechanical Engineering, National Cheng Kung University, No.1, University Road, Tainan 701401, Taiwan

that surface roughness had an oscillating decrease as overlap ratio increased. Zhong et al. [4] mentioned that porosity decrease occurs with laser power increasing or powder feed rate decreasing. Deposition rate and powder usage ratio both increase with laser power increasing, but only deposition rate increases as powder feed rate increasing, powder usage ratio had an opposite trend. Scanning speed had no obvious effect on porosity, deposition rate and powder usage ratio. Gao et al. [5] adjusted laser defocus distance to conduct DED experiments; from the results, they found that when the laser defocus distance was set below the deposition surface, the laser energy distribution was more uniform and the qualities of deposited product was better. Ma et al. [6] proposed that the defocus was the most significant parameter on dilution which had nearly a linear effect. Zheng et al. [7] results show that the accumulation of un-melted powder particles on the side walls of deposited sections can be avoided by selecting a laser under-focused condition. In this study, laser defocus was chosen as one of the process parameters. Bhardwaj et al. [8] pointed out that the main challenge in laser deposition of metallic powders on a substrate is he selection of a suitable range of the involved process parameters. D.R. Feenstra et al. [9] results showed that laser power, scan speed and powder supply rate were the most influential parameters. Guo et al. [10] found that the laser power and overlap ratio are significant to the flatness ratio. Therefore, this study considered overlap ratio as our control factor as well.

In order to analyze the impacts of multiple factors on qualities more efficiently and comprehensively, many DoE methods which has been widely used in other fields [11–13] were gradually applied in DED researches. Ng et al. [14] used response surface methodology to conduct experiments and combined with ANOVAs to study the effects of process factors on the porosity of DED products. Qi et al. [15] selected the width and height of DED single-track product as the qualities to perform factors screening experiments and used central composite design method to design experiments. Found out significant factors and build regression model. Then used laser power to achieve the width control of single-track DED product and finished blade repairments. Lee et al. [16] investigated the effects of process parameters on deposited single-track geometry. The cross-sectional profile of the deposited bead was analyzed to understand the effects of each process condition on the bead geometry. Moreover, a mathematical formula for bead geometry prediction was derived using the RSM, which can be used to effectively control the process variables to achieve the desired qualities. Sheshadri et al. [17] conducted the Taguchi experiment determine optimal levels resulting in better surface quality and microhardness. Lian et al. [18] used Taguchi-Grey relational analysis to design experiments in order to optimize deposition rate and product surface flatness of single-layer multi-track DED products. The obtained optimal factor setting can simultaneously improve the two qualities.

After reviewing the research results mentioned above, it can be found that most scholars focused on the influences of factors on single quality and tried to figure out the mechanisms. However, it was rarely mentioned that how to adjust factor setting when multiple qualities of a DED product conflict with each other. Although Lian et al. [18] used Taguchi-Grey relational analysis to design and conduct multi-objective optimization research, their optimization targets only chose deposition rate and surface roughness. Cladding efficiency and porosity, which are closely related to the cost of powder materials and the mechanical strength of the products, are also extremely important qualities and need to be optimized.

So, the biggest goal of this research was finishing a multi-objective optimization by using Taguchi-Grey relational analysis as DoE method. Laser power, overlap ratio, powder feed rate, scanning speed and laser defocus distance were selected as the control factors of DoE in order to optimize cladding efficiency, surface roughness and porosity of DED products. The variation trends of each quality were investigated when the control factors were varied and the optimal factor setting which can simultaneously take the three qualities into account was found. ANOVAs were also conducted to find out significant factors of each qualities. By using the significant factors as variations, three second-order polynomial regression predictive models for qualities were built.

Furthermore, according to the GRA and ANOVAs results, two OFAT experiments which used the optimal setting as the center point were performed. Adjusted the overlap ratio and laser defocus distance of the optimal setting and investigated the three qualities variations. Then, the OFAT experiment results were used to verified the accuracies of three qualities regression models.

2 Materials and methods

2.1 Equipment and materials

IPG YLS-3000 fiber laser with 1070 nm wavelength and 3000 W maximum power was used in this research. The laser spot diameter was 3 mm, and it had a flat-top energy distribution. The used Precitec YC30 laser head was coaxial four-way powder feeding type and it had a hub which can used to adjust the laser focus position. GTV PF 2/2 LC powder feeder was used to transport metal powder to the laser head. It had a rotating powder disk and transporting unit was rpm. It was measured that 1 rpm was equivalent to 10.08 g/min. The laser head was installed on Tongtai TMV-710A

Table 1 IN 718 powder composition

Element	Ni	Cr	Fe	Nb	Mo	Ti	Al
Wt%	52.51	17.78	Bal.	5.14	3.06	1.00	0.54

machine tool which equipped with a double rotary table and can perform five-axis simultaneous movement.

The powder and substrates materials used in this study were both nickel-based superalloy IN 718. This alloy presents excellent properties at high-temperature applications (useful up to 980°C), oxidation, and corrosion-resistant properties, and it is widely used in the aeronautical sector [19]. The dimensions of the substrate were: L100 x W100 x H15 mm. The IN 718 powder was generated by gas atomization. The particle size distribution range of the powder was 53-150 μm. The composition of this powder is shown in Table 1.

2.2 Design of Taguchi experiment

Taguchi method is a multivariate experiment design method. Through mathematical and statistical tools, it helps researchers more effectively to study relations between multi-level control factors and product quality and find an optimal factor setting.

In order to fabricate solid products, firstly it is necessary to ensure the quality of single layer deposition. Therefore, this study used a flat rectangle as experiment product (as shown in Fig. 1), and chose laser power, overlap ratio, powder feed rate, scanning speed and laser defocus distance as control factors to design the Taguchi experiment. Optimized DED product qualities of single-layer and multi-track deposition process.

The definition of overlap ratio is shown below and in Fig. 2.

$$\text{Overlap ratio} = \frac{W - H}{W} \cdot 100\% \quad (1)$$

where

W: Width of single track
H: Hatching space

The laser defocus distance means the relative distance between the laser focus (F_L) and deposition surface (F_S) under the premise that the positions of powder focus (F_P) and F_S are the same. As shown in Fig. 3, positive/negative refers to the position above/below F_S and the value refers to the distance.

In this Taguchi experiment, it was assumed that there was no strong interaction between the control factors. L_{16} orthogonal array was used to design the Taguchi experiment with five four-level control factors and it was repeated three times (as shown in Tables 2 and 3).

2.3 Product properties and Signal-to-Noise Ratio (SNR) criteria

Cladding efficiency, surface roughness and porosity were chosen as the optimization target qualities in this research. The definitions, calculation and measurement approaches of each quality are show below.

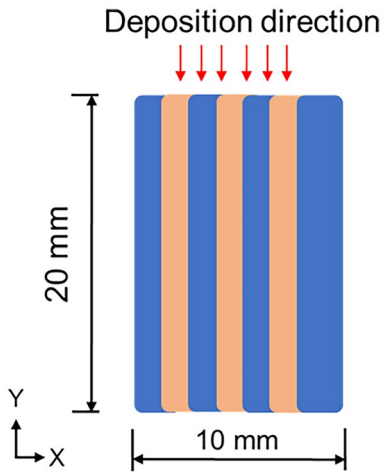

Fig. 1 Schematic of Taguchi experiment product deposition

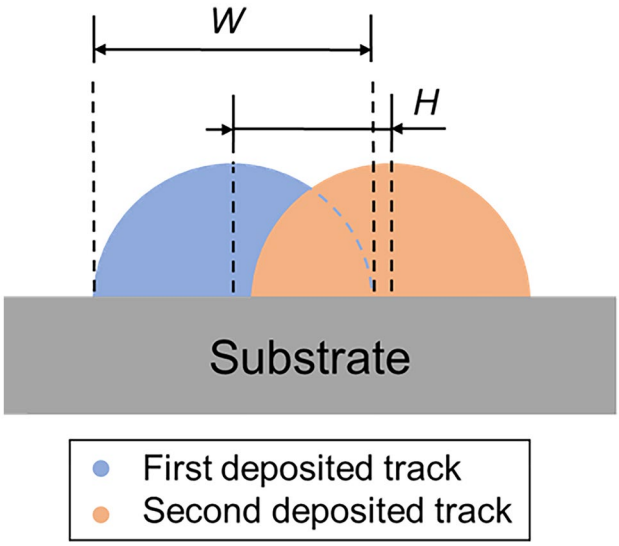

Fig. 2 Schematic of multi-track deposition

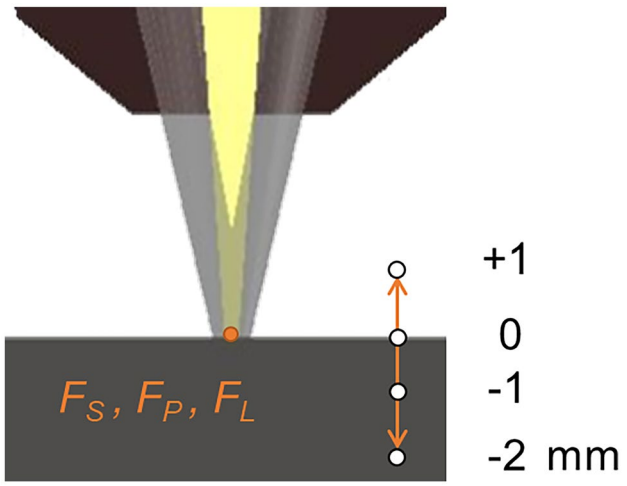

Fig. 3 Schematic of the setting of laser defocus distance

(1) Cladding efficiency (*CE*)

$$CE = \frac{W_{\text{clad}}}{W_{\text{feed}}} \cdot 100\% \tag{2}$$

where W_{clad}: Increase of substrate weight after cladding. W_{feed}: Weight of input powder which is equal to the product of powder feed rate and cladding time.

The SNR conversion criterion of *CE* was large-the-better (LTB). Its formula is:

$$\eta_1 = \eta_{LTB} = -10 \cdot \log\left[\frac{1}{n}\sum_{i=1}^{n}\left(\frac{1}{y_i}\right)^2\right] \tag{3}$$

where η_1: SNR of cladding efficiency. y_i: Measurement value of i-th experiment. n: Experiment repeated times.

(2) Surface roughness (S_a)

Bruker's ContourGT-K white light interferometer was used to measure the surface roughness of top surface of deposited products. The used measurement criterion was arithmetic mean height of the surface (*Sa*). The SNR conversion criterion of Sa was smaller-the-better (STB). Its formula is:

$$\eta_2 = \eta_{STB} = -10 \cdot \log\left[\frac{1}{n}\sum_{i=1}^{n} y_i^2\right] \tag{4}$$

Table 3 L_{16} orthogonal array

	A Laser power (W)	B Overlap ratio (%)	C Powder feed rate (rpm)	D Scanning speed (mm/s)	E Laser defocus (mm)
1	800	30	0.7	4	−2
2	800	40	1	7	−1
3	800	50	1.3	10	0
4	800	60	1.6	13	1
5	1000	30	1	10	1
6	1000	40	0.7	13	0
7	1000	50	1.6	4	−1
8	1000	60	1.3	7	−2
9	1200	30	1.3	13	−1
10	1200	40	1.6	10	−2
11	1200	50	0.7	7	1
12	1200	60	1	4	0
13	1400	30	1.6	7	0
14	1400	40	1.3	4	1
15	1400	50	1	13	−2
16	1400	60	0.7	10	−1

where η_2: SNR of surface roughness.

(3) Porosity (P_t)

After depositions, specimens were cut along the cross section of the parts by WEDM. Then, the specimens were grinded and polished with sandpaper and diamond slurry. Used Leica DM6000M optical microscope to take images of the specimens (at 7.5 magnification times), and the image analysis software Image J was used to calculate the area of pores in the specimen cross sections (as shown in Fig. 4).

The calculation formula of the porosity is shown in (2.3–2.4), and it also used small-the-better SNR conversion criterion.

$$P_t = \frac{\sum_{i=1}^{n} A_i}{A_c + A_M} \cdot 100\% \tag{5}$$

where $\sum_{i=1}^{n} A_i$: Sum of cross section area of pores. A_c: Cross section area of deposited material. A_M: Cross section area of melt pool.

Table 2 Control factors and its level values

Notation	Factor	Level 1	Level 2	Level 3	Level 4
A	Laser power (W)	800	1000	1200	1400
B	Overlap ratio (%)	30	40	50	60
C	Powder feed rate (rpm)	0.7	1	1.3	1.6
D	Scanning speed (mm/s)	4	7	10	13
E	Laser defocus distance (mm)	−2	−1	0	1

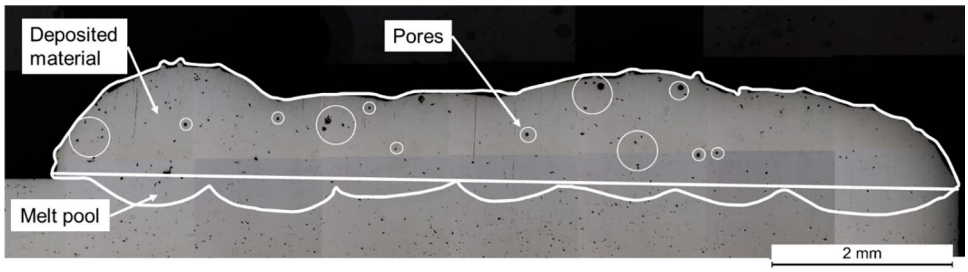

Fig. 4 An image of specimen cross section

$$\eta_3 = \eta_{\mathrm{STB}} = -10 \cdot \log\left[\frac{1}{n}\sum_{i=1}^{n} y_i^2\right] \tag{6}$$

where η_3: SNR of porosity.

After finishing Taguchi experiments and SNRs analysis, ANOVAs were conducted to assess the effect levels of control factors on the three qualities, and found the most significant control factors. The significant factors were used as variables to create second-order polynomial regression models of three qualities.

2.4 Grey relational analysis

Taguchi method can optimize "one" quality and find the optimal factor setting. However, the DED optimization problem in this research is a "multi-objective" optimization problem. In order to take all qualities into account at the same time and try not to be biased, this research used Grey relational analysis (GRA) method based on Taguchi experiment to find the optimal factor setting. There are three steps in Grey relational analysis:

(1) Grey relation generating The action of processing various data with different order levels and making them comparable is "Grey relation generation." Considering the characteristic of SNR, the SNRs of three qualities were normalized to [0,1]. The normalization formula is shown in Eq. 7. Figure 5 shows the procedure diagram of GRA.

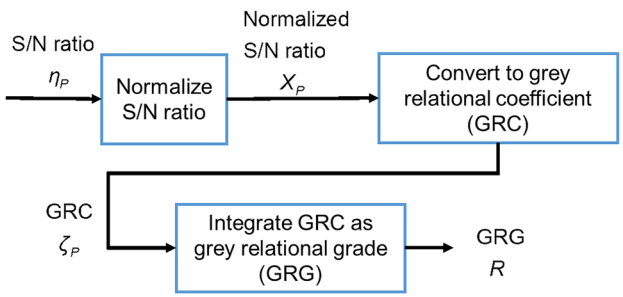

Fig. 5 GRA procedure diagram

$$X_P(i) = \frac{\eta_P(i) - \min\left(\eta_P(i)\right)}{\max\left(\eta_P(i)\right) - \min\left(\eta_P(i)\right)} \tag{7}$$

where $\eta_P(i)$: SNR of P-th quality of i-th experiment run. $X_P(i)$: Normalized SNR of P-th quality of i-th experiment run. P: 1,2 and 3 (which present CE, S_a and P_t) i: 1, 2,..., 16

(2) Grey relational coefficient (GRC) calculation Then convert the normalized SNRs into the Grey correlation coefficient.

$$\zeta_P(i) = \frac{\min|1 - X_P(i)| + \psi \cdot \max|1 - X_P(i)|}{|1 - X_P(i)| + \psi \cdot \max|1 - X_P(i)|} = \frac{0 + \psi \cdot 1}{|1 - X_f(i)| + \psi \cdot 1} \tag{8}$$

where $\zeta_P(i)$: GRC ψ: Distinguishing coefficient ($\psi = 0.5$)

(3) Grey relational grade (GRG) calculation Finally, the three GRCs were integrated as GRG with the same weight value.

$$R(i) = \sum_{P=1}^{L_p} \beta_P \cdot \zeta_P(i) \tag{9}$$

where R(i): GRG of i-th experiment run. β_P: Weight value (in this study, all weight values were $\frac{1}{3}$).

After the above three steps, three SNRs were integrated as one GRG. Then, it could follow Taguchi method to analyze the control factors and find the optimal factor setting.

3 Results and discussion

After three repeated Taguchi experiments, the images of some deposited products are shown in Fig. 6. The average Taguchi experiment results and the converted SNR are shown in Table 4:

3.1 Cladding efficiency

Table 5 and Fig. 7 which were made by the cladding efficiency SNR (η_1) data of Table 4 show the effect levels on η_1 of control factors.

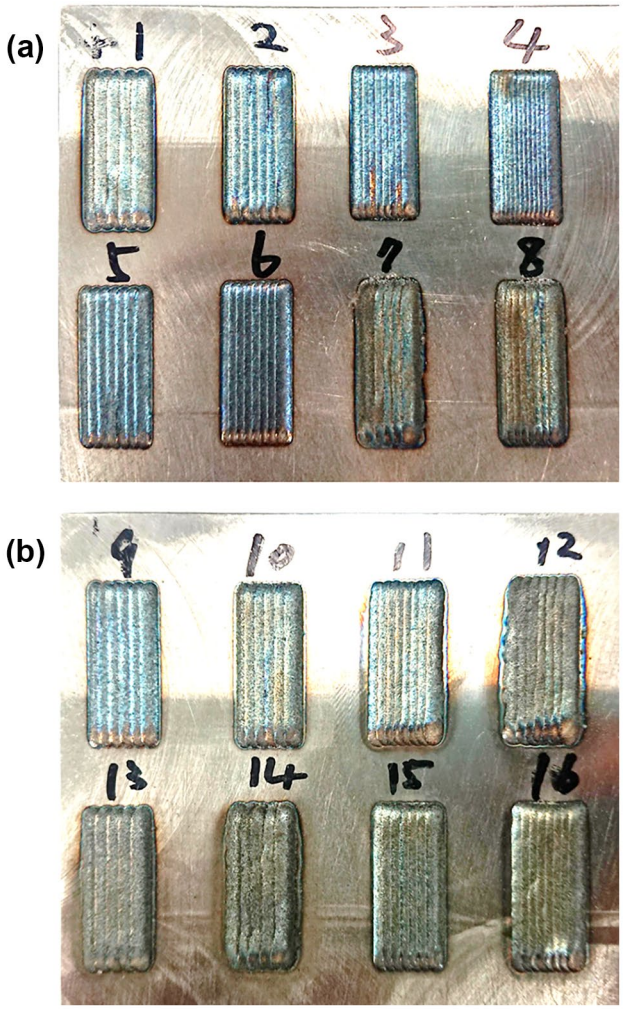

Fig. 6 Deposited products of Taguchi experiments

As shown in Table 5, the effect level order of factors is: powder feed rate (C) > laser power (A) > laser defocus distance (E) > overlap ratio (B) > scanning speed (D). According to the levels which each factor can get the highest η_1, the optimal factor setting that can get the best deposition efficiency is: $A_4\,B_1\,C_1\,D_3\,E_1$.

In Fig. 7, η_1 increases when laser power and scanning speed increase. The reasons are listed following. (1) The laser power increase makes the input powder more likely to be melt and deposited. (2) The scanning speed increase has a greater effect on reduction of powder input per unit time. However, this study used the concept of powder usage to define the cladding efficiency; the reduction of powder input amount will relatively increase the percentage of powder which can be melt by constant laser power. So, the cladding efficiency increases as scanning speed increases.

In addition,η_1 decreases when overlap ratio, powder feed rate and laser defocus distance increase. The reasons are listed following. (1) The larger overlap ratio the smaller the hatching space. It will increase the probability of powder hitting old tracks and rebounding. (2) The powder that can be melt by the laser is limited, and the excessive powder is difficult to be melt and used, which resulting in lower cladding efficiency. (3) As the study of Gao et al. [5], when Gaussian laser is set at negative defocus position, the energy distribution of the beam spot section is relatively even. This phenomenon should be the same in the flat-top laser used in this study. Then, when the laser defocus distance increases from negative to positive, the energy density at the edge of the spot decreases sharply and reduce the percentage of powder usage.

3.2 Surface roughness

Table 6 and Fig. 8 which were made by the surface roughness SNR (η_2) data of Table 4 show the effect levels on η_2 of control factors.

As shown in Table 6, the effect level order of factors is: scanning speed (D) > powder feed rate (C) > overlap ratio (B) > laser power (A) > laser defocus distance (E). According to the levels which each factor can get the highest η_2, the optimal factor setting that can get the best surface roughness is: $A_2\,B_4\,C_2\,D_4\,E_3$.

In Fig. 8, η_2 increases when overlap ratio and scanning speed increase and decreases when powder feed rate increases. However, when the laser power and laser defocus distance increase, the value of η_2 oscillates in a small range without significant change.

The variation trend that surface roughness becomes better when overlap ratio increase is consistent with the research results of Li and Ma [3]. When the powder feed rate increases, if input powder be deposited successfully, the single track will have a larger aspect ratio and contact angle. This characteristic will result in a rough top surface of product when the single tracks overlap track by track. By contrast, the scanning speed increases will reduce the amount of powder input per unit time and lets the single track with a low aspect ratio. So, its multi-track product will have better surface roughness.

3.3 Porosity

Table 7 and Fig. 9 which were made by the porosity SNR (η_3) data of Table 4 show the effect levels on η_3 of control factors.

As shown in Table 7, the effect level order of factors is: laser power (A) > laser defocus distance (E) > powder feed rate (C) > scanning speed (D) > overlap ratio (B). According to the levels which each factor can get the highest η_3, the optimal factor setting that can get the lowest porosity is: $A_4\,B_4\,C_1\,D_1\,E_4$.

Table 4 Qualities and SNRs of Taguchi experiment products

Run	A	B	C	D	E	Cladding efficiency (%)	Surface roughness (μm)	Porosity (%)	SNR		
	Laser power (W)	Overlap ratio (%)	Powder feed rate (rpm)	Scanning speed (mm/s)	Laser defocus (mm)				Cladding efficiency	Surface roughness	Porosity
1	800	30	0.7	4	−2	57.26%	47.82	0.34%	−4.893	−33.622	49.265
2	800	40	1	7	−1	44.64%	29.98	0.35%	−7.224	−29.583	49.059
3	800	50	1.3	10	0	41.55%	32.06	0.43%	−7.640	−30.270	47.186
4	800	60	1.6	13	1	33.79%	22.65	0.28%	−9.426	−27.361	51.085
5	1000	30	1	10	1	43.93%	28.16	0.24%	−7.228	−29.053	52.339
6	1000	40	0.7	13	0	54.12%	20.46	0.23%	−5.476	−26.279	52.575
7	1000	50	1.6	4	−1	36.58%	44.81	0.21%	−8.789	−33.032	53.484
8	1000	60	1.3	7	−2	45.07%	35.20	0.35%	−6.977	−30.945	49.079
9	1200	30	1.3	13	−1	55.39%	34.74	0.48%	−5.137	−31.335	46.206
10	1200	40	1.6	10	−2	55.29%	31.17	0.39%	−5.164	−30.103	47.496
11	1200	50	0.7	7	1	53.94%	28.75	0.10%	−5.438	−29.628	59.651
12	1200	60	1	4	0	45.92%	35.13	0.12%	−6.782	−30.964	57.259
13	1400	30	1.6	7	0	47.74%	39.18	0.14%	−6.424	−31.932	56.452
14	1400	40	1.3	4	1	50.98%	54.48	0.11%	−6.095	−34.813	58.446
15	1400	50	1	13	−2	64.48%	22.76	0.25%	−3.833	−27.275	51.654
16	1400	60	0.7	10	−1	66.43%	24.56	0.08%	−3.608	−28.147	60.487

Table 5 The average cladding efficiency SNR ($\overline{n_{1\_FK}}$) obtained at the condition of F factor and K level

	A	B	C	D	E
Level 1	−7.296	−5.920	−4.854	−6.640	−5.217
Level 2	−7.117	−5.990	−6.267	−6.516	−6.189
Level 3	−5.630	−6.425	−6.462	−5.910	−6.580
Level 4	−4.990	−6.698	−7.451	−5.968	−7.047
Range	2.306	0.778	2.597	0.730	1.830

Table 6 The average surface roughness SNR ($\overline{\eta_{2\_FK}}$) obtained at the condition of F factor and K level

	A	B	C	D	E
Level 1	−30.21	−31.49	−29.42	−33.11	−30.49
Level 2	−29.83	−30.19	−29.22	−30.52	−30.52
Level 3	−30.51	−30.05	−31.84	−29.39	−29.86
Level 4	−30.54	−29.35	−30.61	−28.06	−30.21
Range	0.714	2.131	2.622	5.045	0.663

In Fig. 9, η_3 increases when laser power, overlap ratio and laser defocus distance increase. The reasons are listed following. (1) Increasing laser power can melt powder more completely. According to Tatsuhiko Kuriya et al. research [1], a larger amount of heat prolongs the solidification time of melt pool, allowing the bubbles to escape and reducing the porosity of the product. (2) In addition, a higher overlap ratio means that the hatching space between the tracks is short. The old deposited track will continue to be affected by the heat of the new track, and it will also increase the probability of bubbles escaping. (3) Because laser energy at the positive defocus will be more concentrated in the center [3], it leads to a higher temperature and prolong the time for the bubbles to leave.

Besides, η_3 decreases when powder feed rate and scanning speed increase. The reasons are listed following. (1) The more powder input, the more laser energy will be dispersed. It will cause the temperature of the overall deposit to drop and reduce the time required for solidification. It results in more air bubbles in products.

3.4 ANOVA results of properties

The ANOVA results of cladding efficiency SNR (η_1) are shown in Table 8. In this study, one-half rule was used, which selects the first three control factors having the highest contribution to the variation of η_1 as significant factors. Then, the overlap ratio (B) and scanning speed (D) which had lower effect level were pooled as the experiment error to calculate F-values and confidence levels.

The confidence levels for the significance of laser power (A), powder feed rate (C) and laser defocus distance (E) are 98.86%, 98.53% and 94.16%, respectively, showing that these three factors have significant influences on η_1 variation. Their contributions of to the η_1 variation are 38.58%, 34.73% and 18.35%. Compared with the experiment error (pooled B and D factors), which accounts for 8.34%, A, C and E factors have significant effects on cladding efficiency.

The ANOVA results of surface roughness SNR (η_2) are shown in Table 9. Similarly, one-half rule was used, and the laser power (A) and laser defocus distance (E) were pooled as the experiment error to calculate F-values and confidence levels.

The confidence levels for the significance of overlap ratio (B), powder feed rate (C) and scanning speed (D) are 98.26%, 99.62 and 99.98%, respectively, showing that these three factors have significant influences on η_2 variation. Their contributions of to the η_2 variation are 11.21%, 20.85% and 65.05%. Compared with the experiment error (pooled A and E factors), which accounts for 2.89%, B, C and D factors have significant effects on surface roughness.

The ANOVA results of porosity SNR (η_3) are shown in Table 10. Since the effects of the five factors on η_2 are closer, only the overlap ratio (B) which has the lowest significance was pooled as the experiment error to calculate the F-value and confidence levels.

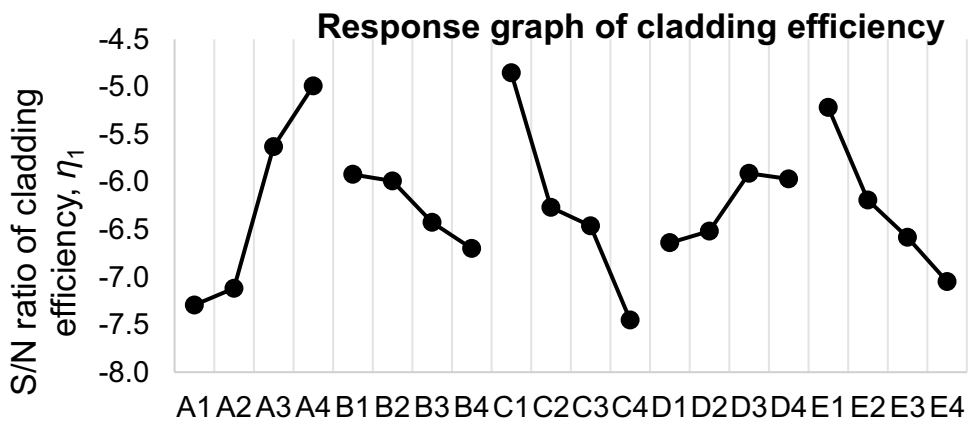

Fig. 7 Response graph of cladding efficiency SNR (η_1)

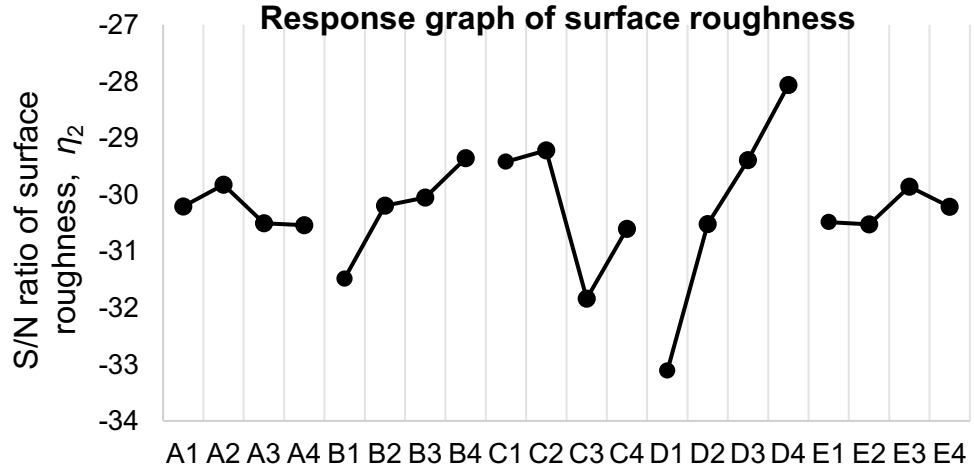

Fig. 8 Response graph of surface roughness SNR (η_2)

Table 7 The average porosity SNR ($\overline{\eta_{3\_FK}}$) obtained at the condition of F factor and K level

	A	B	C	D	E
Level 1	49.149	51.066	55.495	54.614	49.373
Level 2	51.869	51.894	52.578	53.560	52.309
Level 3	52.653	52.994	50.229	51.877	53.368
Level 4	56.760	54.478	52.129	50.380	55.380
Range	7.611	3.412	5.265	4.234	6.007

The confidence levels for the significance of laser power (A), powder feed rate (C), scanning speed (D) and laser defocus distance (E) are 94.54%, 80.82%, 71.38% and 87.49%, respectively, showing that these four factors have significant influences on η_3 variation. Their contributions of to the η_3 variation are 37.31%, 17.83%, 13.08% and 23.59%. Compared with the experiment error (pooled B factors), which accounts for 8.19%, A, C, D and E factors have significant effects on porosity.

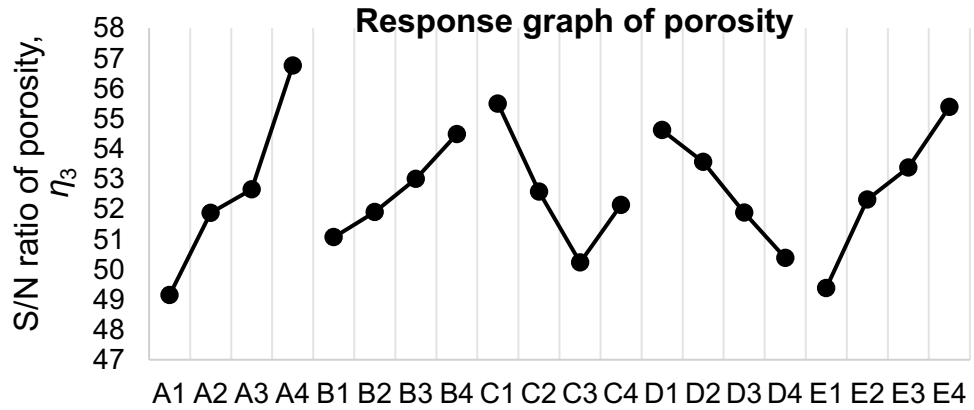

Fig. 9 Response graph of porosity SNR (η_3)

Table 8 The ANOVA results of η_1

ANOVA of cladding efficiency S/N ratio						
Factor	SS	DOF	Var	F-Value	Confidence level	Contribution
A	15.267	3	5.089	9.253	98.86%	38.58%
B	Pooled					
C	13.742	3	4.581	8.329	98.53%	34.73%
D	Pooled					
E	7.260	3	2.420	4.400	94.16%	18.35%
Error	3.300	6	0.550	-	-	8.34%
Total	39.569	15	-	-	-	100%

Table 9 The ANOVA results of η_2

ANOVA of surface roughness S/N ratio						
Factor	SS	DOF	Var	F-Value	Confidence level	Contribution
A	Pooled					
B	9.480	3	3.160	7.752	98.26%	11.21%
C	17.643	3	5.881	14.427	99.62%	20.85%
D	55.034	3	18.345	45.001	99.98%	65.05%
E	Pooled					
Error	2.446	6	0.408	-	-	2.89%
Total	84.603	15	-	-	-	100%

3.5 Regression models

Based on the results of ANOVAs, this study took the significant factors of each quality as variables, and established a second-order polynomial regression model. However, the units and magnitudes of levels of these factors were not the same. Before building the regression model, the levels of control factors were all normalized to [−1,1], but their respective distributions of level values were still the same.

$$U_{N\alpha\_FK} = \frac{U_{FK} - \mu_F}{\mathrm{Max}\left(U_{FK}\right) - \mathrm{Min}\left(U_{FK}\right)} \in [-1, 1] \tag{10}$$

where $U_{N\alpha\_FK}$: Normalized i-th level of a control factor. U_{FK}: The i-th level of a control factor before normalization. μ_F: Average of level values of a control factor.

Table 11 shows L_{16} array with normalization control factors and the average measurement value of qualities.

The following are the regression prediction equations of the three qualities.

$$\begin{aligned} CE = {} & 45.75 + 13.73 \cdot A - 14.38 \cdot C - 9.23 \cdot E \\ & + 10.19 \cdot A \cdot C - 12.06 \cdot A \cdot E - 5.56 \cdot C \cdot E \\ & + 14.92 \cdot A^2 + 7.42 \cdot C^2 + 6.96 \cdot E^2 \end{aligned} \tag{11}$$

$$\begin{aligned} S_a = {} & 31.61 - 7.86 \cdot B + 6.68 \cdot C - 19.66 \cdot D \\ & - 6.35 \cdot B \cdot C + 10.34 \cdot B \cdot D - 0.88 \cdot C \cdot D \\ & + 2.11 \cdot B^2 - 12.54 \cdot C^2 + 22.17 \cdot D^2 \end{aligned} \tag{12}$$

$$\begin{aligned} P_t = {} & 0.3084 - 0.2186 \cdot A + 0.1459 \cdot C + 0.2661 \cdot D \\ & - 0.094 \cdot E + 0.0212 \cdot A \cdot C + 0.1865 \cdot A \cdot D \\ & + 0.4765 \cdot A \cdot E + 0.2216 \cdot C \cdot D - 0.0609 \cdot C \cdot E \\ & - 0.22 \cdot D \cdot E - 0.0712 \cdot A^2 - 0.2089 \cdot C^2 - 0.0941 \cdot E^2 \end{aligned} \tag{13}$$

The R^2 values of regression models of cladding efficiency and surface roughness are 0.9105 and 0.8806. It means that the regression models using the significant control factors of the two qualities as the variables have good ability to present the experiment results. So, the two regression models can be used to primarily predict cladding efficiency and surface roughness of DED products.

The R^2 value of porosity regression model which is created by using four control factors as variables is 0.9745. It means that the porosity model has great ability to present the experiment results. However, the extremely high R^2 of this model may also be caused by the model overfitting. Because there were four variables used to build porosity regression model (the others have three variables), only 16 pieces of data obtained from L_{16} experiment may be not enough. To

Table 10 The ANOVA results of η_3

ANOVA of porosity S/N ratio						
Factor	SS	DOF	Var	F-Value	Confidence level	Contribution
A	119.003	3	39.668	4.553	94.54%	37.31%
B	Pooled					
C	56.880	3	18.960	2.176	80.82%	17.83%
D	41.709	3	13.903	1.596	71.38%	13.08%
E	75.261	3	25.087	2.880	87.49%	23.59%
Error	26.135	3	8.712	-	-	8.19%
Total	318.988	15	-	-	-	100%

Table 11 L_{16}array after control level normalization and measurement result

Run	Laser power, A	Overlap ratio, B	Powder feed rate, C	Scanning speed, D	Laser defocus distance, E	Average *CE* (%)	AverageS_a(μm)	AverageP_t(%)
1	−0.500	−0.500	−0.500	−0.500	−0.500	57.26%	47.82	0.34%
2	−0.500	−0.167	−0.167	−0.167	−0.167	44.64%	29.98	0.35%
3	−0.500	0.167	0.167	0.167	0.167	41.55%	32.06	0.43%
4	−0.500	0.500	0.500	0.500	0.500	33.79%	22.65	0.28%
5	−0.167	−0.500	−0.167	0.167	0.500	43.93%	28.16	0.24%
6	−0.167	−0.167	−0.500	0.500	0.167	54.12%	20.46	0.23%
7	−0.167	0.167	0.500	−0.500	−0.167	36.58%	44.81	0.21%
8	−0.167	0.500	0.167	−0.167	−0.500	45.07%	35.20	0.35%
9	0.167	−0.500	0.167	0.500	−0.167	55.39%	34.74	0.48%
10	0.167	−0.167	0.500	0.167	−0.500	55.29%	31.17	0.39%
11	0.167	0.167	−0.500	−0.167	0.500	53.94%	28.75	0.10%
12	0.167	0.500	−0.167	−0.500	0.167	45.92%	35.13	0.12%
13	0.500	−0.500	0.500	−0.167	0.167	47.74%	39.18	0.14%
14	0.500	−0.167	0.167	−0.500	0.500	50.98%	54.48	0.11%
15	0.500	0.167	−0.167	0.500	−0.500	64.48%	22.76	0.25%
16	0.500	0.500	−0.500	0.167	−0.167	66.43%	24.56	0.08%

confirm whether there is an overfitting problem, it needs to test the model with additional experiment data.

Therefore, this study used additional experiment data to test the predictive abilities of cladding efficiency and surface roughness regression models and whether there is an overfitting problem in porosity model. This part will be presented and discussed in Sect. 4.3.

3.6 Grey relational analysis

In 3.1–3.3 sections, the analysis results of Taguchi experiment show that the optimal factor settings of cladding efficiency, surface roughness and porosity are $A_4\ B_1\ C_1\ D_3\ E_1$, $A_2\ B_4\ C_2\ D_4\ E_3$ and $A_4\ B_4\ C_1\ D_1\ E_4$, respectively. Obviously, the optimal settings of each quality are not

Table 12 L_{16}array showing GRA data processing procedures

Run	S/N ratio			Normalization of S/N ratio			GRC			GRG
	CE	S_a	P_t	*CE*	S_a	P_t	*CE*	S_a	P_t	(R)
1	−4.893	−33.622	49.265	0.779	0.140	0.214	0.694	0.368	0.389	0.483
2	−7.224	−29.583	49.059	0.379	0.613	0.200	0.446	0.564	0.385	0.464
3	−7.640	−30.270	47.186	0.307	0.532	0.069	0.419	0.517	0.349	0.42
4	−9.426	−27.361	51.085	0.000	0.873	0.342	0.333	0.798	0.432	0.520
5	−7.228	−29.053	52.339	0.378	0.675	0.429	0.446	0.606	0.467	0.506
6	−5.476	−26.279	52.575	0.679	1.000	0.446	0.609	1.000	0.474	0.694
7	−8.789	−33.032	53.484	0.109	0.209	0.510	0.360	0.387	0.505	0.417
8	−6.977	−30.945	49.079	0.421	0.453	0.201	0.463	0.478	0.385	0.442
9	−5.137	−31.335	46.206	0.737	0.408	0.000	0.655	0.458	0.333	0.482
10	−5.164	−30.103	47.496	0.733	0.552	0.090	0.652	0.527	0.355	0.511
11	−5.438	−29.628	59.651	0.685	0.608	0.941	0.614	0.560	0.895	0.689
12	−6.782	−30.964	57.259	0.454	0.451	0.774	0.478	0.477	0.689	0.547
13	−6.424	−31.932	56.452	0.516	0.338	0.717	0.508	0.430	0.639	0.525
14	−6.095	−34.813	58.446	0.573	0.000	0.857	0.539	0.333	0.778	0.549
15	−3.833	−27.275	51.654	0.961	0.883	0.381	0.928	0.811	0.447	0.728
16	−3.608	−28.147	60.487	1.000	0.781	1.000	1.000	0.696	1.000	0.898
Max	−3.608	−26.279	60.487	-	-	-	-	-	Avg. ($\bar{R}$)	0.555
Min	−9.426	−34.813	46.206	-	-	-	-	-	-	

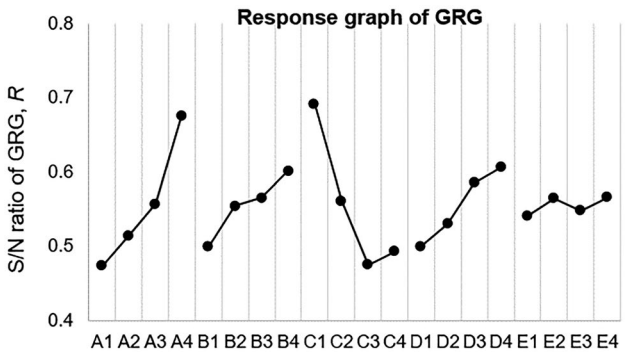

Fig. 10 Response graph of GRG (R)

Table 13 The GRG obtained at the condition of F factor and K level

	A	B	C	D	E
Level 1	0.474	0.499	0.691	0.499	0.541
Level 2	0.514	0.555	0.561	0.530	0.565
Level 3	0.557	0.565	0.475	0.585	0.549
Level 4	0.675	0.602	0.493	0.606	0.566
Range	0.201	0.103	0.216	0.107	0.025

the same, and variation trends caused by a control factors for different qualities are even opposite. Therefore, this study based on the Taguchi experiment data, used Grey relational analysis to help to achieve the goal of simultaneously optimizing the three qualities. As mentioned in Sect. 2.4, the Grey relational analysis is divided into three steps to process the SNRs and convert the "three" qualities into "one" composite index (Grey relational grade, GRG). So, the DED process quality can be comprehensively evaluated and the optimal factor setting for all qualities can be determined.

After calculating the GRG (as shown in Table 12), the study followed Taguchi's method again to make a factor response graph to analyze the effects of control factors on the variation of GRG.

As shown in Fig. 10 and Table 13, the effect level order of factors is: powder feed rate (C) > laser power (A) > scanning speed (D) > laser defocus distance (E) > overlap ratio (B). According to the levels which each factor can get the highest R, the optimal factor setting that can get the highest GRG is: $A_4\,B_4\,C_1\,D_4\,E_4$.

Similarly, this study also performed an ANOVA for GRG (the results are shown in Table 14). the degree of overlap B and the laser defocus distance E, which have a less obvious impact on the variance of R, are combined (Pooled) as the experimental error (Error). The overlap ratio (B) and laser defocus distance (E) which had lower effect level were pooled as the experiment error.

The laser power (A), powder feed rate (C) and scanning speed (D) are the significant factors of which confidence levels for the significance are 98.22%, 98.98% and 83.96%, respectively. Their contributions to the R variation are 38.12%, 44.44% and 11.27%

4 Verification and one-factor-at-a-time experiments

4.1 Verification of optimized factor setting

After finishing Taguchi-Grey relational analysis and obtaining the optimal factor setting ($A_4\,B_4\,C_1\,D_4\,E_4$), in order to verify the effectiveness of it, this study used it to deposit the 20x10 mm^2 flat rectangle product again and compared its deposition result with the one which is deposited by using laboratory previous setting for a thin-walled cylinder part. (laser power (A) 1000 W, powder supply (C) 1.1 rpm, scanning speed (D) 7 mm/s and laser defocus distance (E) −2 mm) In addition, the overlap ratio (B) was set as 60% which was equal to the optimal factor setting.

The two settings were deposited once, respectively, and the comparisons between their deposition results are shown as following. (Due to COVID-19 epidemic, the verification experiment used Nikon 10x optical microscope to take cross-sectional images as shown in Fig. 11.)

Table 14 The ANOVA results of R

ANOVA of GRG						
Factor	SS	DOF	Var	F	Confidence level	Contribution
A	0.091	3	0.030	7.662	98.22%	35.12%
B	Pooled					
C	0.115	3	0.038	9.697	98.98%	44.44%
D	0.029	3	0.010	2.460	83.96%	11.27%
E	Pooled					
Error	0.024	6	0.004	-	-	9.17%
Total	0.258	15	-	-	-	100%

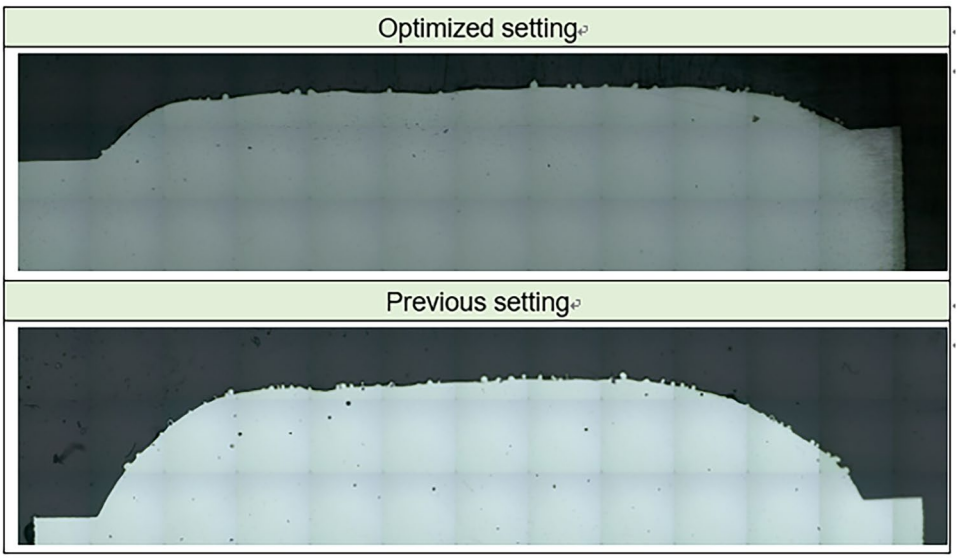

Fig. 11 Cross section images of the verification experiment

It can be seen from the above comparison results shown in Table 15. The optimal setting $A_4\,B_4\,C_1\,D_4\,E_4$ had better qualities of DED product compared with the previous setting. It shows that the new factor setting can effectively improve the product qualities of the DED process in single-layer multi-track deposition.

4.2 One-factor-at-a-time experiment results

This study found an optimal factor setting $A_4\,B_4\,C_1\,D_4\,E_4$ for a single-layer and multi-track DED process that can take three qualities into account. However, 3D parts need to be stacked with multiple layers and often have different appropriate deposition toolpaths for different part geometries. They are the problems that the optimal factor setting for general single-layer and multi-track deposition need to face.

The overlap ratio (B) and laser defocus distance (E) are the most change-demanding control factors. The overlap ratio has a directly influence on the time span required for a part to be deposited. According to the literature review and laboratory past research [20], when the laser defocus distance is an appropriate negative value, the laser focus will provide a self-repairing function to eliminate the uneven surface of last layer. It is due to when the laser focus on negative defocus position passes through uneven surface, the focus will close to lower positions and away from higher positions.

Therefore, based on the ANOVA results of the GRG, the study adjusted the overlap ratio (B) and laser defocus distance (E) to conduct an one-factor-at-a-time (OFAT) experiment. The OFAT experiment did not change the significant factors, maintaining the level of laser power (A), powder feed rate (C) and scanning speed (D) at $A_4\,C_1\,D_4$. Similarly, using flat rectangle as experiment product, observed the variation trends of product qualities. Expecting when the significant factors were fixed, the quality variations caused by adjusting the overlap ratio and laser defocus distance will not be severe. So, the factor setting can flexibly adjust the two factors depending on different fabrication requirements. Using $A_4\,B_4\,C_1\,D_4\,E_4$ as the center setting, the OFAT experiment results are shown in Table 16.

It can be seen from the above OFAT experiment results (as shown in Figs. 12, 13 and 14) that except for the cladding efficiency having greater variation, the effects of adjusting overlap ratio and laser defocus distance on the surface roughness and porosity is relatively insignificant, both values oscillating in a small range. The variation trend of the cladding efficiency in the OFAT experiment is also the same as the analysis result in Sect. 3.1, which when the overlap ratio and laser defocus distance increase, the cladding efficiency has decreasing trends.

Combining the results of OFAT experiment and laboratory past research, the laser defocus distance is

Table 15 Qualities comparison results of the verification experiment

	Cladding efficiency		Surface roughness		Porosity	
	CE (%)	η_1	S_a (μm)	η_2	P_t (%)	η_3
Optimized setting	61.41%	−4.235	13.99	−22.916	0.036%	68.938
Previous setting	47.35%	−6.494	30.34	−29.640	0.088%	61.096

Table 16 Results of OFAT experiment

	Run	Laser power (W)	Overlap ratio (%)	Powder feed rate (rpm)	Scanning speed (mm/s)	Laser defocus distance (mm)	Cladding efficiency (%)	Surface roughness (μm)	Porosity (%)
Optimized setting	1	1400	60	0.7	13	1	61.41%	13.99	0.036%
OFAT setting	2	1400	50	0.7	13	1	65.64%	20.09	0.025%
	3	1400	40	0.7	13	1	73.70%	15.90	0.025%
	4	1400	30	0.7	13	1	69.09%	21.63	0.040%
	5	1400	60	0.7	13	0	55.27%	22.44	0.060%
	6	1400	60	0.7	13	−1	62.18%	13.57	0.078%
	7	1400	60	0.7	13	−2	76.00%	16.47	0.039%

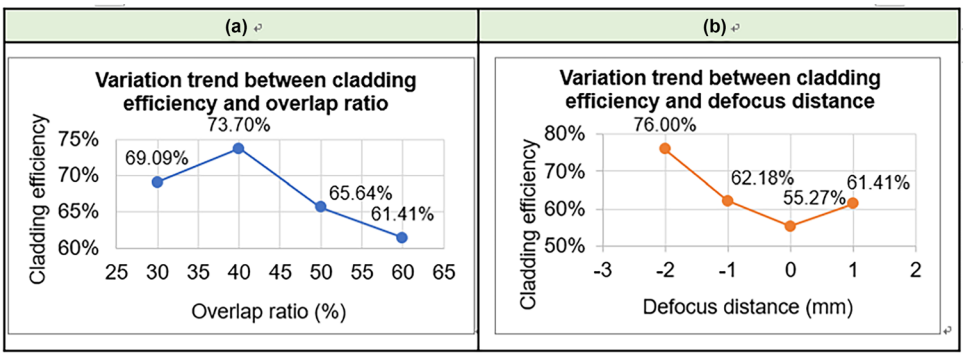

Fig. 12 Variation trends of cladding efficiency under adjusting **a** overlap ratio and **b** laser defocus distance

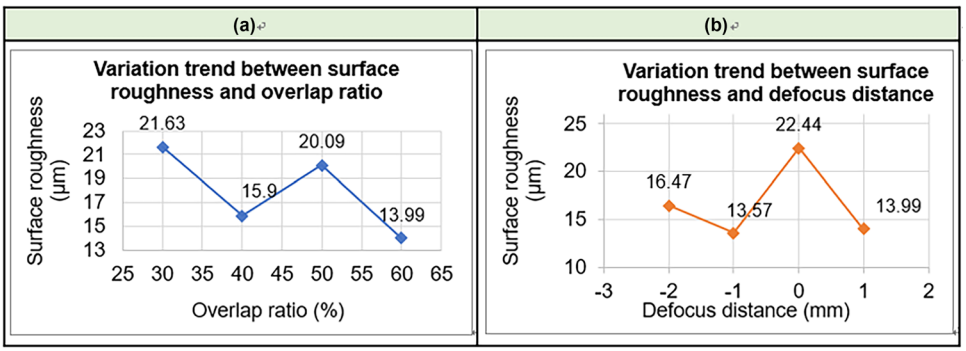

Fig. 13 Variation trends of surface roughness under adjusting **a** overlap ratio and **b** laser defocus distance

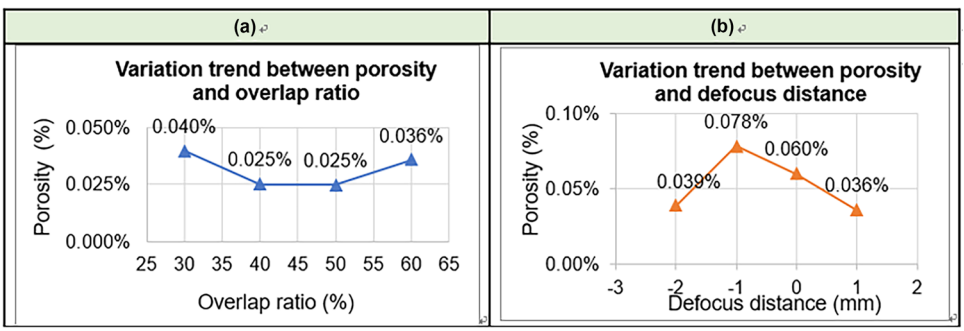

Fig. 14 Variation trends of porosity under adjusting **a** overlap ratio and **b** laser defocus distance

recommended to set as −2 mm (E1) based on cladding efficiency and the overlap degree was set as 30% (B1). So, the setting $A_4 B_1 C_1 D_4 E_1$ can maintain high cladding efficiency and low processing time.

4.3 Verifications of Regression Models

As mentioned in Sect. 3.5, additional experiment data are needed for comparison in order to know the predictive ability of qualities regression models. Therefore, this study compared the OFAT and verification experiment results with the predictive values of the regression models. The results are shown in Table 17. Since the regression models of cladding efficiency and porosity did not use the overlap ratio (B) as variable, the predicted values of the OFAT experiment runs using overlap ratio as independent variable were all the same. In the same way, the surface roughness model had a constant predictive value for the runs that used the laser defocus distance (E) as the independent variable in the OFAT experiment.

In Table 17, the average error between the predictive and experiment values of cladding efficiency is 9.98%, which can be said that the cladding efficiency regression model has good prediction accuracy. The average predictive error of the surface roughness model is 24.22%. The errors between predictive experiment values of each run are oscillating and the variation of predictive values is small. This shows that the predictive surface roughness has stabilized in this interval, but its oscillation amplitude is smaller than the actual measured value. Although not as accurate as the cladding efficiency model, this surface roughness model can still provide a predictive value as a reference when adjusting process factors.

The average predictive error of the porosity regression model is a very large value, 358%. It can be said that the accuracy of the prediction of the porosity model is not satisfactory. Comparing with its 0.9745 R^2 value, the "model overfitting" problem mentioned in Sect. 3.5 is revealed.

From the ANOVA results of porosity in Sect. 3.4, except for the laser power, the difference in effects of the other four factors on the porosity variation are not obvious. It means that these four factors may have similar significance and no one can be discarded. However, the Taguchi L_{16} array can only produce 16 data. If use five factors for quadratic polynomial regression, the correct regression equation cannot be obtained due to insufficient simultaneous equations.

When draw the predictive and OFAT experiment values of porosity in the same line graph (as shown in Fig. 15), it can be observed that they have a similar variation trends during independent variables changing. Therefore, whether the experiment data are sufficient should be considered to avoid model overfitting problem. Then, the regression approach can have better prediction ability.

Table 17 Results of qualities comparison

	Run	Cladding efficiency (%)			Surface roughness (μm)			Porosity (%)		
		Predictive value	Experiment result	Error	Predictive value	Experiment result	Error	Predictive value	Experiment result	Error
Optimized setting	1	58.35	61.41	4.99%	21.84	13.99	56.13%	0.184	0.0357	415%
OFAT setting	2	58.35	65.64	11.11%	21.21	20.09	5.59%	0.184	0.0247	645%
	3	58.35	73.70	20.83%	21.05	15.90	32.40%	0.184	0.0249	638%
	4	58.35	69.09	15.55%	21.36	21.63	1.25%	0.184	0.0397	363%
	5	60.96	55.27	10.29%	21.84	22.44	2.66%	0.183	0.0600	205%
	6	65.12	62.18	4.72%	21.84	13.57	60.96%	0.16	0.0782	107%
	7	70.82	76.00	6.81%	21.84	16.47	32.62%	0.119	0.0390	206%
Previous setting	8	49.99	47.35	5.57%	31.00	30.34	2.18%	0.340	0.0881	286%
			Avg.	9.98%		Avg.	24.22%		Avg.	358%

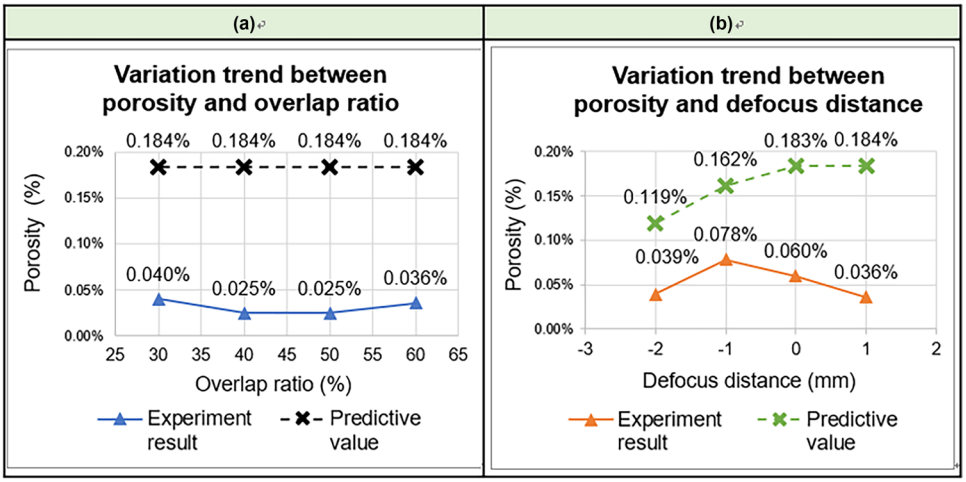

Fig. 15 Predictive and experiment porosity values at using **a** overlap ratio and **b** laser defocus distance as independent variables OFAT experiment

5 Conclusion

In this study, Taguchi L_{16} array was used to design the five four-level factor deposition experiments, and three product qualities were obtained and converted into SNR for factor response analyses and ANOVAs. In addition, a one-factor experiment was used to further explore the non-significant factors and verify the accuracy of the model. The final analysis results came to the following conclusions:

(1) According to the analysis results, the most significant factors of cladding efficiency were: laser power, powder feed rate and laser defocus distance. The cladding efficiency increased when the laser power increased and decreased when the powder feed rate and laser defocus distance increased.
(2) The factors that had the most significant effect on the surface roughness were: the overlap ratio, powder feed rate and scanning speed. The surface roughness became better when the overlap ratio and scanning speed increased, and got worse when powder feed rate increased.
(3) The porosity was significantly affected by the laser power; however, the difference between the significances of the other four factors were not very obvious. Therefore, only the overlap ratio which had the lowest significance was considered as insignificant factor. The porosity decreased with the laser power and laser defocus distance increasing and increased with the powder feed rate and scanning speed increasing.
(4) Using Grey relational analysis to combine the three qualities into the Grey relational grade (GRG) and used it as a composite index to find the optimal factor setting: $A_4\,B_4\,C_1\,D_4\,E_4$. The results of ANOVA for the GRG showed that the laser power, powder supply and scanning speed were the most significant factors.
(5) In order to realize the flexibility and stability of optimal setting when it faces with different DED process applications, this study additionally used the overlap ratio and laser defocus distance as the independent variables to conduct the OFAT experiment. As its results, when adjusted the two factors, besides that the cladding efficiency had large variation, both the values of surface roughness and porosity oscillated in a small range. Therefore, considering cladding efficiency and processing time, this study recommended to use $A_4\,B_1\,C_1\,D_4\,E_1$ as the main factor setting and apply it to workpiece manufacturing in future path planning research.
(6) The Taguchi experiment data were used to build the regression models of three qualities by using their significant factors as variables. After comparing the experiment values obtained from the OFAT experiment, the results showed that the cladding efficiency and surface roughness regression model both had predictive capabilities. They were sufficient to be used as a tool for preliminary prediction of product quality.
(7) The porosity model had big error between its predictive and experiment values due to model over fitting problem. It was necessary to increase the number of samples to increase the accuracy of the regression model.

Author contributions All authors contributed to the study conception and design. Material preparation, data collection and analysis were performed by [Yu-Yang Chang], [Jun-Ru Qiu] and [Sheng-Jye Hwang]. The first draft of the manuscript was written by [Yu-Yang Chang] and all authors commented on previous versions of the manuscript. All authors read and approved the final manuscript.

Funding The authors declare that no funds, grants, and other support were received during the preparation of this manuscript.

Availability of data and material Not applicable.

Code availability Not applicable.

Declarations

Ethics approval The authors confirm the novelty of the reported work and confirm that it is not submitted to any other journal.

Consent to participate The authors give consent to participate.

Consent for publication The authors give consent for publication.

Conflicts of interest The authors have no relevant financial or non-financial interests to disclose. On behalf of all authors, the corresponding author states that there is no conflict of interest.

References

1. Kuriya T, Koike R, Mori T, Kakinuma Y (2018) Relationship between solidification time and porosity with directed energy deposition of Inconel 718. J Adv Mech Des Syst Manuf 12(5):0104–0104
2. Liu Z, Kim H, Liu W, Cong W, Jiang Q, Zhang H (2019) Influence of energy density on macro/micro structures and mechanical properties of as-deposited Inconel 718 parts fabricated by laser engineered net shaping. J Manuf Process 42:96–105
3. Li Y, Ma J (1997) Study on overlapping in the laser cladding process. Surf Coat Technol 90(1–2):1–5
4. Zhong C, Biermann T, Gasser A, Poprawe R (2015) Experimental study of effects of main process parameters on porosity, track geometry, deposition rate, and powder efficiency for high deposition rate laser metal deposition. J Laser Appl 27(4):042003
5. Gao W, Zhao S, Liu F, Wang Y, Zhou C, Lin X (2014) Effect of defocus manner on laser cladding of Fe-based alloy powder. Surf Coat Technol 248:54–62
6. Ma M, Xiong W, Lian Y, Han D, Zhao C, Zhang J (2020) Modeling and optimization for laser cladding via multi-objective quantum-behaved particle swarm optimization algorithm. Surf Coat Technol 381:125129
7. Zheng B, Haley J, Yang N, Yee J, Terrassa K, Zhou Y, Lavernia E, Schoenung J (2019) On the evolution of microstructure and defect control in 316l SS components fabricated via directed energy deposition. Mater Sci Eng A 764:138243
8. Bhardwaj T, Shukla M, Paul C, Bindra K (2019) Direct energy deposition-laser additive manufacturing of titanium-molybdenum alloy: Parametric studies, microstructure and mechanical properties. J Alloy Compd 787:1238–1248
9. Feenstra D, Molotnikov A, Birbilis N (2021) Utilisation of artificial neural networks to rationalise processing windows in directed energy deposition applications. Mater Des 198:109342
10. Guo C, He S, Yue H, Li Q, Hao G (2021) Prediction modelling and process optimization for forming multi-layer cladding structures with laser directed energy deposition. Opt Laser Technol 134:106607
11. Asghar A, Abdul Raman AA, Daud WMAW (2014) A comparison of central composite design and Taguchi method for optimizing Fenton process. Sci World J 2014
12. Jou Y-T, Lin W-T, Lee W-C, Yeh T-M (2014) Integrating the Taguchi method and response surface methodology for process parameter optimization of the injection molding. Appl Math Inf Sci 8(3):1277
13. Pan LK, Wang CC, Wei SL, Sher HF (2007) Optimizing multiple quality characteristics via Taguchi method-based Grey analysis. J Mater Process Technol 182(1–3):107–116
14. Ng G, Jarfors A, Bi G, Zheng H (2009) Porosity formation and gas bubble retention in laser metal deposition. Appl Phys A 97(3):641–649
15. Qi H, Azer M, Singh P (2010) Adaptive toolpath deposition method for laser net shape manufacturing and repair of turbine compressor airfoils. Int J Adv Manuf Technol 48(1–4):121–131
16. Lee EM, Shin GY, Yoon HS, Shim DS (2017) Study of the effects of process parameters on deposited single track of M4 powder based direct energy deposition. J Mech Sci Technol 31(7):3411–3418
17. Sheshadri R, Nagaraj M, Lakshmikanthan A, Chandrashekarappa MPG, Pimenov DY, Giasin K, Prasad RVS, Wojciechowski S (2021) Experimental investigation of selective laser melting parameters for higher surface quality and microhardness properties: Taguchi and super ranking concept approaches. J Market Res 14:2586–2600
18. Lian G, Zhang H, Zhang Y, Tanaka ML, Chen C, Jiang J (2019) Optimizing processing parameters for multi-track laser cladding utilizing multi-response grey relational analysis. Coatings 9(6):356
19. Ramiro P, Ortiz M, Alberdi A, Lamikiz A (2020) Geometrical model and strategy in single and multilayer structures deposited by powder-fed directed energy deposition. Procedia CIRP 94:352–356
20. Lin P-Y, Shen F-C, Wu K-T, Hwang S-J, Lee H-H (2020) Process optimization for directed energy deposition of ss316l components. Int J Adv Manuf Technol 111(5):1387–1400